1 **Testing the performance of one and two box models as tools for risk assessment**

2 **of particle exposure during packing of inorganic fertilizer**

3 Carla Ribalta[1,2], Antti J. Koivisto[3], Ana López-Lilao[4], Sara Estupiñá[4], María C.

4 Minguillón[1], Eliseo Monfort[4], Mar Viana[1].

5 [1]Institute of Environmental Assessment and Water Research (IDÆA-CSIC), C/ Jordi Girona 18, 08034

6 Barcelona, Spain.

7 [2]Barcelona Univeristy, Chemistry Faculty, C/ de Martí i Franquès, 1-11, 08028 Barcelona, Spain

8 [3]National Research Centre for the Working Environment, Lersø Parkallé 105, Copenhagen DK-2100,

9 Denmark.

10 [4]Institute of Ceramic Technology (ITC)- AICE - Universitat Jaume I, Campus Universitario Riu Sec, Av.

11 Vicent Sos Baynat s/n, 12006 Castellón, Spain.

12 **Highlights:**

13 • Occupational exposure to particles during industrial packing was assessed.

14 • No significant increases were found during packing of a granulate fertilizer.

15 • One and two box models predicted adequately actual worker exposure.

16 • Including outdoor concentrations in models was seen to improve their

17 performance.

18 • Models parametrization was seen to be a key issue to adequately predict

19 exposure.

20 **Abstract**

21 Modelling of particle exposure is a useful tool for preliminary exposure assessment in

22 workplaces. However, actual exposure measurements are needed to assess models

23 reliability. Worker exposure was monitored during packing of a complex inorganic

24 granulate fertilizer at industrial scale using small and big bags. Particle concentrations

25 were modelled with one and two box models, where the emission source was

26 estimated with the fertilizer's dustiness index. The exposure levels were used to

27 calculate inhaled dose rates and test accuracy of the exposure modellings. The particle

number concentrations were measured from worker area by using a mobility and optical particle sizer which were used to calculate surface area and mass concentrations. The concentrations in the worker area during pre-activity ranged from 63797 - 81073 cm^{-3}, $4.6x10^6$ to $7.5x10^6$ um^2 cm^{-3}, and 354 to 634 µg m^{-3} (respirable mass fraction) and during packing from 50300 to 85949 cm^{-3}, $4.3x10^6$ to $7.6x10^6$ um^2 cm^{-3}, and 279 to 668 µg m^{-3} (respirable mass fraction). Thus, the packing process did not significantly increase the exposure levels. High particle number concentration was partly due to the use of diesel-powered forklifts. The particle surface area deposition rate in respiratory tract was up to $7.6x10^6$ $µm^2$ min^{-1} during packing, with 52% - 61% of deposition occurring in the alveolar region. Ratios of the modelled and measured concentrations were 0.98 ± 0.19 and 0.84 ± 0.12 for small and big bags, respectively, when using the one box model, and 0.88 ± 0.25 and 0.82 ± 0.12, respectively, when using the two box model. The modelling precision improved for both models when outdoor particle concentrations were included. This study shows that exposure concentrations during packing of fertilizers can be predicted with a reasonable accuracy by using a concept of dustiness and mass balance models.

Keywords: indoor aerosol modelling, exposure prediction, occupational exposure, industrial packing, risk management.

1. Introduction

Industrial bag filling, packing and pouring processes have been pointed out as activities with high potential to emit airborne particles. Studies in different industrial sectors had reported high levels of worker exposure to particles, e.g; during pouring and packing of paint pigments, packing of TiO_2, carbon black, fullerenes and carbon nanofibres (Ding et al., 2017; Fujitani et al., 2008; Koivisto et al., 2015, 2012a; Koponen et al., 2015; Kuhlbusch et al., 2004, Evans et al., 2010) as well as packing and pouring of cement materials (Notø et al., 2018; Peters et al., 2008). Additionally, differences in particle

release have been observed when pouring different materials, different amounts, and using different types of mixing tanks (Koponen et al., 2015). Thus, every case is specific and further research is needed in order to understand emission patterns during packing and pouring.

Exposure to particulate matter (PM) is known to cause various adverse health effects, such as pulmonary and cardiovascular diseases and cancer (Landrigan et al., 2017). Current epidemiological and toxicological studies consider $PM_{2.5}$ (with aerodynamic particle diameter $D_p \leq 2.5$ µm) as the most harmful component for human health (Gakidou et al., 2017; Landrigan et al., 2017; World Health Organization, 2016). Inorganic complex fertilizers have been found to be moderately toxic to earthworms (Shruthi et al., 2017). In humans, due to inhalation of fertilizer degradation products, health effects might come up especially after long term exposures (Yara Iberian S.A, 2005). Ammonium nitrate, used in complex inorganic fertilizers, when inhaled, was seen to cause possibly meaningful pulmonary function changes (Kleinman et al., 1980) and to be irritating, cause coughing, bronchospasm, laryngospasm and laryngeal edema even at low concentrations (Gorguner and Akgun, 2003). Additionally, the clinical examination of workers of the ammonium nitrate production showed frequent cases of chronic bronchitis and radiculoneuropathy (Tsimakuridze et al., 2005). On the other hand, ammonium nitrate is known to be potentially explosive when confined. Potassium nitrate, also included in some inorganic fertilizers composition, has been seen to be irritating for the respiratory tract (INCHEM, 2001). Therefore, the study of packing of an inorganic fertilizer is of interest as workers can be exposed to relatively high concentrations of airborne fertilizer particles, which might cause respiratory health effects.

Exposure prediction models have been proposed as valuable risk assessment tools. Since the initial application of exposure prediction models, several research papers

have been published regarding their theoretical aspects (Ganser and Hewett, 2017; Hewett and Ganser, 2017; Hussein and Kulmala, 2008; Nazaroff, 2004; Nazaroff and Cass, 1989). The two box model is a well-accepted exposure assessment tool in the risk assessment field as, even with its simplified assumptions, it is able to adequately simulate actual conditions for various processes including volatile compounds and PM emissions (Arnold et al., 2017; Jayjock et al., 2011). In the chemical industry, models have been tested in a variety of cases (Nicas, 2016; Sahmel et al., 2009 and references therein). However, when testing the models for PM in actual industrial environments, the number of studies decreases (Arnold et al., 2017; Boelter et al., 2009; Johnson et al., 2011; Jones et al., 2011; Koivisto et al., 2015; Lopez et al., 2015). Recently, Arnold et al. (2017) conducted a study where the one and two box models, were evaluated under highly controlled conditions. Predicted exposure results for three industrial solvents when using near and far field models was categorized excellent and good to excellent under the ASTM Standard 5157 criteria (Arnold et al., 2017). However, in order to implement prediction models as trustable tools for worker risk assessment, additional real-world cases need to be evaluated to test model performance and to understand the uncertainties related to critical parameters, such as the source characterization, local controls, and air mixing (Jayjock et al., 2011; Sahmel et al., 2009).

The objectives of the present study were 1) to perform a worker exposure and risk assessment study of packing of an inorganic complex fertilizer in an industrial plant, and 2) to test the one box and two box models performance in real-world settings in order to contribute to the better understanding and validation of exposure prediction models.

2. Methodology

2.1. Work environment and packing process

The measurements were carried out during packing of a fertilizer in two different packing lines between the 23th and 26th of January 2017 at an industrial facility located in Castellón, Spain. The fertilizer (YaraMila COMPLEX, PF595P, YaraIberian S.A.) main components were ammonium nitrate; NH_4NO_3 (15 - 20%), potassium nitrate; KNO_3 (12.5 - 15%) and calcium fluoride; CaF_2 (2 - 3%). The fertilizer was granulated in 2.5 to 5 mm diameter spherical pellets.

The packing hall was only naturally ventilated and the replacement air came from outdoors and from adjacent industrial hall via doors, which were always open (Figure 1). The packing lines were for small bags (25 kg) and big bags (600 kg) where the studied fertilizer was poured into the bags from a silo by using a feed funnel. Figure S1 in the Supporting Information shows photos from the packing lines. The two packing lines were not operated at the same time. Two-day measurements were conducted at both packing lines, small bags day 1 (SB1), small bags day 2 (SB2), big bags day 1 (BB1) and big bags day 2 (BB2). In small bags, packing was carried out through an opening fitting the bag width (33-35 cm) and subsequently mechanically sealed. The fertilizer was poured at a flow of 250 kg min^{-1} and the drop height was 5 cm from the feed funnel to the bag opening. Total material drop height was approximately 0.6 m. The packing process was fully automated and the process area was partially enclosed. In big bags, packing was carried out through a cylindrical opening (20 cm diameter) and at a 175 kg min^{-1} flow; material drop height was 20 cm from the feed funnel to the bag opening. Total material drop height was approximately 1.3 m. In that case, the bag was manually closed by the worker, who was standing in front of the bag at approximately 0.5 m distance.

132 During small and big bags filling, workers tasks were to control and guarantee the
133 correct functioning of the lines as well as to move the filled bags to the storage area
134 using an electric forklift. Occasionally, diesel-powered forklifts were performing truck
135 loading and unloading operations in the hall.

136 **2.2. Aerosol measurements and sampling**

137 Particle number and mass concentrations were monitored in real time in the worker
138 area (WA), indoors, and outdoors (Figure 1). All online instruments were synchronized
139 prior to the measurements and intercompared overnight between experiments. Particle
140 concentrations during packing were measured for approximately two hours.
141 Additionally, 30 minutes of pre-activity concentrations were measured for each day
142 except for BB2.

143 In the worker are, the instruments were placed on a portable table at approximately 1
144 m height (instrument inlets being at 1.5 m above the ground level), at 0.5 m from the
145 emission source and 1 m from the worker (Figure 1 and Figure S1, Supporting
146 Information). The monitoring instruments were:

147 - An electrical mobility spectrometer (NanoScan, SMPS TSI Model 3910; sample
148   flow rate 0.7 l min^{-1}) to measure particle number concentration and particle size
149   distribution in 13 channels from 10 to 420 nm with a 1 minute time resolution
150 - A Mini Wide Range Aerosol Spectrometer (Mini-WRAS 1371; sample flow rate
151   1.2 l min^{-1}) to measure particle mass concentration, particle number
152   concentration and particle size distribution from 10 nm to 35 μm in 41 channels
153   with a 1 minute time resolution
154 - A miniature diffusion size classifier (DiSCmini Matter Aerosol, Testo; sample
155   flow rate 1 l min^{-1}) to measure particle number concentration, mean particle size
156   and alveolar lung deposition surface area (LDSA) in a range of 10 to 700 nm
157   with a 1 minute time resolution

158   -   A Mini Laser Aerosol Spectrometer (Grimm, Mini-LAS 11R; sample flow rate 1.2

159   l min^{-1}) to measure particle mass concentration from 0.25 to 32 µm in 31

160   channels with a 1 minute time resolution.

161   The indoor and outdoor concentrations were monitored by using a DiSCmini and a

162   Grimm Mini-LAS, with the same settings as described above.

163   During the packing process, particles emitted were collected onto Au grids (Quantifolil

164   ® with 1 µm diameter holes – 4 µm separation of 200 mesh). The grids were attached

165   to polycarbonate filters that were placed in a sampling cassette (SKC INC., USA, inlet

166   diameter 1/8 in. and filter diameter 25 mm). The cassette was connected to a Leland

167   pump with an operating flow rate of 3 l min^{-1}. The morphology and primary particle size

168   of the particles collected were determined using a transmission electron microscope

169   (TEM, Jeol, JEM 1220, Tokyo, Japan) coupled with an energy-dispersive X-ray (EDX)

170   spectrometer.

171   The worker area particle number size distributions measured by the NanoScan and

172   MiniWras were combined according to Koivisto et al. (2012a) to obtain a wide range for

173   particle size distribution from 10 nm to 35 µm. NanoScan size channels between 11.5 -

174   86.6 nm were used while channels ranging from 139 nm to 35 µm were taken from the

175   MiniWras. Between 86.6 nm and 139 nm a combined channel (108.6 nm) was created.

176   Upper channels from NanoScan (> 115.5 nm) were not used as it is known to not have

177   a good resolution for particles >200 nm (Fonseca et al., 2016), while MiniWras was

178   seen to not accurately measure particles under 50 nm; therefore, MiniWras lower

179   channels were not used (see Figure S2, Supporting information) and explanation.

180   Here, due to channels cut, ultrafine particles are defined as D_p < 86.60 nm, fine

181   particles as 86.60 nm < Dp < 943.0 nm and coarse particles as > 943.0 nm.

182 Increases and reductions in exposure during packing when comparing with pre-activity

183 levels were considered statistically significant when the following approach (Asbach et

184 al., 2012; Kaminski et al., 2015) was fulfilled:

185

186 Mean concentration during packing > BG ± 3*(σBG)

187

188 where BG is the mean temporal background (pre-activity) concentration and σBG is the

189 standard deviation of the background concentration.

190 **2.3. Dustiness**

191 Material dustiness was assessed by using the continuous drop standard method (EN

192 15051). The continuous drop device, made of stainless steel, consisted of a cylindrical

193 pipe through which air circulated in an upward direction with a volume flow rate of 53 l

194 min^{-1}. Concentric to the cylindrical pipe there was an inner pipe, slightly shorter than

195 the cylindrical pipe, through which material was dropped at a flow rate of 6 to 10 g min-

196 ^{1}, so that the powdered material was released into a counter-current airflow (López-

197 Lilao et al., 2015). Total material drop height during the test is approximately 1.2 m.

198 Two sampling heads for inhalable (approximately PST; designed by Institut für

199 Gefahrstoff-Forschung-IGF) and respirable (approximately PM_4; FSP-2, BGIA) fractions

200 were located slightly above the discharge position of the material. Samples for

201 gravimetric measurements of inhalable and respirable fractions were collected on

202 cellulose thimbles, single thickness, 10x50 mm 25/pk and PVC filters of 37 mm and 5

203 mc of porosity respectively. The experiment, which lasted for 10 minutes, was repeated

204 two times to ensure results repeatability. Between experiment repetitions, the sampling

205 heads for inhalable and respirable fractions were superficially cleaned while the rest of

206 the device was thoroughly cleaned only at the end of the test.

207

2.4. Exposure modelling

2.4.1. Dispersion models

Exposure modelling was performed by using a one box model (Hewett and Ganser, 2017) and a two box model (Ganser and Hewett, 2017). Figure 2 shows the models schemes and the mass balance equations. The models assume that 1) particles are fully mixed at all times; 2) mass is created by a source inside the plant (near field in two box model) and by concentrations coming from outdoors; 3) there are no other particle losses than the natural ventilation. The models were used to calculate the respirable fraction. Particle losses by sedimentation may be considered negligible for this size fraction.

2.4.2. Emission source

The emission (S) from the packing process is described based on the dustiness index as:

$$S(t) = DI \cdot H \cdot \frac{dM(t)}{dt} \cdot LC \qquad (1)$$

where DI is the respirable dustiness index of the fertilizer expressed in mg kg^{-1} or particles kg^{-1}, H is the handling energy factor for the process, dM/dt (kg min^{-1}) is the mass flow of the fertilizer, and LC is the protection factor of localized controls. The respirable dustiness index of the fertilizer was obtained using the continuous drop method, as it is the method that adapts better to the process under study (Pujara, 1997; Ribalta et al., 2018 under review).

2.4.3. Modelling parametrization

The input parameters needed to run the model and experimentally unavailable in this case study are the handling energy factor (H), local control factors (LC), and the air flow rate (β) between near field (NF) and far field (FF) (for two box model only).

232   By definition, H, links the energy applied during the process with the energy applied

233   during the dustiness test and can range from 0 to 1 (Koivisto et al., 2015; Lidén, 2006;

234   Schneider and Jensen, 2007). Here, H was set to 0.5 for small bags because the drop

235   height during small bags packing was ca. half of the drop height in dustiness test. For

236   big bags, H was assumed to be 1 as material drop height was similar to dustiness drop

237   height (see 2.1 and 2.4). With regard to local controls (LC), two main controls were

238   detected. For both small and big bags, the bag itself was estimated in this work to

239   reduce particle release by 40% (applied in the emission rate equation as (LC_{bag} = 0.6).

240   In addition, for small bags one box model, the effect of the enclosure was taken into

241   account and applied in the model reducing emission by 50% ($LC_{enclosed}$ = 0.5)

242   (Fransman et al., 2008). Finally, β was estimated after testing the range values

243   reported by Baldwin and Maynard (1998) and Arnold et al. (2017) taking into account

244   the characteristics from our case scenarios. A sensitivity analysis for different β was

245   carried out and is reported in the section below (Table 1). For small bags it was set at

246   0.75 m^3 min^{-1} (0.0125 m s^{-1}) as the air flow rate was considered to be low due to the

247   enclosure of the packing line (enclosure opening of 1 m^2). In this case, for the two box

248   model, as the effect of the enclosure was introduced by the NF-FF β, the local control

249   regarding the enclosure ($LC_{enclosed}$) in the emission rate equation was suppressed. For

250   big bags, the air flow rate was considered to be higher as there was no enclosure or

251   division between NF and FF, so β was set to 30 m^3 min^{-1} (0.04 m s^{-1}). The model

252   schemes and parameters are listed in Figure 2. The air exchange rate (AER) between

253   indoor and outdoor air was experimentally calculated considering outdoor wind speed

254   during the measurement period (obtained from the local air quality monitoring network),

255   the size of the outdoors door, and the size of the industrial unit. This resulted in a mean

256   air exchange rate of around 7 h^{-1} for the entire period.

257

258

2.5. Calculated active surface area and mass concentrations

The particle active surface area was calculated by applying particle size distribution obtained from NanoScan and MiniWras data combination to the equation (2) described in Heitbrink et al. (2009) as in Koivisto et al. (2012b).

$$S = \frac{3\pi\lambda D_b}{C_c(D_b)\delta} \qquad (2)$$

where λ is the mean free path for air, 0.066 µm, and δ is the scattering parameter for air, 0.905. D_b is the mobility diameter and C_c the slip correction factor for the corresponding aerodynamic or mobility particle size.

The particle mass was additionally calculated by using mobility particle diameter and effective density as in Koivisto et al. (2012b)

$$m = \rho_{eff} \frac{\pi}{6} D_b^3 \qquad (3)$$

where ρ_{eff} is the effective density. As particles density was unknown, 1 g cm^{-3} was assumed for simplicity.

2.6 Calculated regional inhalation dose rate

The inhalation dose of deposited particles in the respiratory system during inspiration and expiration was quantified. The regional inhalation dose rate was obtained by multiplying particle size concentrations on the worker area (NanoScan and MiniWras data combination) by the ICRP human respiratory tract model deposition probability (ICRP, 2011). The respiratory volume used was 25 I min^{-1}, corresponding to male respiration during light exercise (Koivisto et al., 2012b). The regional dose was calculated for head airways, tracheobronchial and alveolar regions by using simplified deposition fraction equations for the ICRP model as described by Hinds (1999). In the

281 model particles were assumed to be spherical and to preserve their size during
282 inhalation.

3. Results

3.1. Material morphology and characterization

285 Samples collected onto Au TEM grids were observed and characterized using TEM-
286 EDX. In the samples collected during SB2 (Figure 3a, 3b, 3c, 3d and 3e) and
287 BB1(Figure 3f, 3g, 3h and 3i) experiments, particles which main elements were O, Na,
288 K, Ca, Cr and Zn were detected proving the presence of fertilizer particles in the worker
289 area (Figure 3a, 3b, 3c, 3d 3f, 3g and 3h). A few differences were observed between
290 both samples. Fertilizer particles size was between 1 μm up to > 35 μm in both
291 samples, although in BB1 there was a bigger proportion of bigger particles (Figure 3f)
292 whereas in SB2 a bigger proportion of smaller ones (Figure 3c). Additionally,
293 agglomerates of nanoparticles, with particle size < 50nm and main components O and
294 C, were found on both samples indicating the presence in the worker area of diesel
295 combustible particles, coming from the diesel forklift (Figure 3d, 3e, 3h and 3i). Those
296 agglomerates were occasionally seen in the BB1 samples (Figure 3h and 3i), whereas
297 in the SB2 they were highly abundant (Figure 3c, 3d and 3e) owing to a higher activity
298 of diesel forklifts inside the plant (96.2%; Table 2).

3.2. Dustiness indices

300 Material dustiness was assessed using the continuous drop method and results were
301 given in terms of inhalable and respirable mass fractions (mg kg^{-1}) gravimetrically
302 analyzed. Following the EN 15051 dustiness classification for continuous drop, the
303 fertilizer under study was classified as a material with low and very low dustiness
304 indices, with 1026 mg kg^{-1} and 16 mg kg^{-1} for inhalable and respirable fractions,
305 respectively.

12

3.3. Concentrations

3.3.1. Worker area concentrations

The measurements started 34 to 46 minutes prior to the packing process. Packing lasted between 1 h 20 minutes and 2 h 43 minutes (Table 2). For BB2 no background concentrations could be recorded. During SB1 (Figure S3), total particle number and inhalable mass concentrations during packing were similar to background concentrations (Table 3 and Figure S3). Concentrations of fine particles (100 nm - 1 µm) and thoracic and respirable mass concentrations were lower during packing compared with pre-activity levels (Table 3, Figure S3, Supporting information), which resulted from decreasing background concentrations during the pre-activity period (see Figure S3). Thus, it was concluded that during SB1 experiments no significant impacts on particle exposure were detected. Similarly, during SB2 (Figure 4) experiments no statistically significant differences were observed in terms of mass concentrations between the pre-activity and activity periods (Table 3, Figure 4). These results are in agreement with the low dustiness index of the fertilizer material. Conversely, during SB2 total particle number concentration did increase significantly with regard to pre-activity levels (on average for total particle number, 17340 cm^{-3}) (Table 3, Figure 4). This increase may have been linked to diesel emissions from a diesel forklift which operated inside the plant during this period, as will be discussed below. In addition, very few differences were observed in particle size distributions between the pre-activity and activity particle size distributions for SB1 and SB2 (Figure 5a and 5b). In Koivisto et al. (2012a) measurements during packing of TiO_2 into small and large bags did not have an impact on particle concentrations except when opening the enclosed packing machine. Impacts on worker exposure when packing silicon nanoparticles were also not detected probably because the packing line was hermetically sealed (Wang et al., 2012).

During BB1 (Figure 6), particle number and mass concentrations were again similar to pre-activity concentrations, showing slightly higher (non statistically significant) mean concentrations (Table 3).Total particle number concentrations increased by 4876 cm^{-3} and respirable mass concentration by 314 μg m^{-3} (Table 3, Figure 6). During the BB2 (Figure S4) experiments pre-activity concentrations were not available because the activity was initiated before the monitoring instrumentation was ready, and therefore worker exposure can only be discussed comparing with indoor background concentrations. As in the case of SB1 and SB2 very few differences were observed in particle size distribution between the pre-activity and BB1 packing periods. Only slight increases in particles < 30 nm and > 10 μm were observed (Figures 5c). Contrarily, in Koivisto et al. (2012a), packing of TiO_2 into large bags was seen to increase particles > 500 nm. Even so, the present results were to be expected as when classifying the fertilizer according to its dustiness index, it was sorted as a material with very low and low capacity to generate airborne dust for inhalable and respirable fractions, respectively.

As described above, particle number concentrations increased significantly only during two of the four experiments, i.e., SB2 and BB1. However, those increases were not clearly related to the packing activity as no specific relation was seen with the start and stop of the process (Figures 4 and 6). Increases of ultrafine particles in comparison with the background were always below 40000 cm^{-3}, the suggested reference limit value in this specific case (non-biodegradable granular nanomaterials in the range of 1–100 nm and density < 6 kg l^{-1}) (Van Broekhuizen et al., 2012).

Inhalable and respirable mass concentrations did not exceed in any case the limit values for particles not otherwise specified of 10 and 3 mg m^{-3}, respectively (INSH, 2018). Thus, it may be concluded that packing activity of the specific fertilizer did not have a significant impact on worker exposure with regard to particles in the 11.5 nm – 35 μm size range. It should be pointed out that in this study worker exposure

14

concentrations do not correspond strictly to the worker breathing zone (because instruments were not worn by the workers), which are expected to be higher (Koivisto et al., 2015; Koponen et al., 2015). Additionally, the measurements were carried out for a maximum of 2.5 hours and therefore not representative of the 8 hours necessary to calculate the 8 hr time weighted average over a full shift.

Packing processes and similar industrial activities such as material pouring have been previously studied among different types of industries with results indicating that packing, pouring or dumping processes usually lead to slight increases in worker exposure concentrations. Packing of carbon black in bags of 25 kg and 1000 kg was shown to increase airborne particles > 400 nm and mass concentrations (Ding et al., 2017; Kuhlbusch et al., 2004). Fullerenes packing increased particle number > 1000 nm (Fujitani et al., 2008). Evans et al. (2010) also found that dumping of carbon nanofibers into a drum resulted in an increase of respirable mass concentrations. In the case of the cement industry, Notø et al. (2018) found that packing was associated with an increase of worker exposure to the thoracic mass fraction of 12% and 33% when working less than and more than half a shift, respectively. On the contrary, pouring of cement at a construction site was seen to have highly variable and low percentages of inhalable mass exposure, probably because of workers performing pouring operations also carried out other activities (Peters et al., 2008). In comparison to these studies, the fertilizer packing case presented in this work seemed to have one of the lowest impacts on worker exposure to particle mass and number concentrations.

3.3.2. Outdoor concentrations

The packing hall was connected by two doors (Figure 1) to outdoors and to another industrial unit. In both sites other processes were occasionally ongoing. Thus, influence of outdoors and other processes taking place in the adjacent industrial unit were to be expected. Outdoor particle number concentrations as well as PM_{10} mass were usually

385　lower or in a similar range as the worker area and indoor concentrations (thoracic mass

386　fraction) (Table S1 and S2, Supporting information). Regarding mean particle size, it

387　was usually smaller in the outdoor location than in the indoor and worker area by 10 -

388　20 nm (Table S1, Supporting information) due to the influence of outdoor traffic

389　emissions. Mean particle size remained more or less constant between pre-activity and

390　packing periods in the worker area (38-32, 28-37, 33-37, 41-44 nm), indoor (43-37, 38-

391　43 nm) and outdoor (23-20, 31-31, 29-32 nm) measurement points for all days. In

392　general, outdoor concentrations seemed to follow a different pattern from the rest of the

393　locations even if with some exceptions where similar peaks in outdoor, indoor and

394　worker area were observed (e.g., Figure 4, 11:30; Figure S3, 15:10; Figure S4, 12:15).

395　Numerous studies have reported the infiltration of outdoor particles into diverse indoor

396　environments, especially through windows and doors when they are open (Bennett and

397　Koutrakis, 2006; Hussein et al., 2009; Koponen et al., 2001; Reche et al., 2014; Rivas

398　et al., 2015; Wang et al., 2010). In Wang et al. (2010), outdoor infiltration was detected

399　in a similar packing industrial unit where indoor and outdoor areas were connected by

400　opened doors as in the present study.

401　**3.3.3. Forklifts activity**

402　Electric and diesel forklift activity was recorded and is shown on the top of Figures 4, 6,

403　S3 and S4 and as a percentage of total recorded time in Table 2.

404　During the SB1 packing period, an increase in particle number concentration (< 50 nm)

405　was detected when the diesel forklift was driving inside the hall (> 15:00 h) (Figure S3a

406　and S3b). During SB2, only a slight increase in number concentration was observed

407　when the diesel forklift was driving and the electric forklift ended its activity (Figure 4a

408　and 4b, 11:10). During BB1, a slightly increase of particle number concentration (mean

409　size 30 nm) was observed coinciding with the start of a diesel forklift at 10:20 (Figure

410　6a and 6b). During BB2 (Figure S4), two increments of number concentration were

detected, but only the first one could be clearly linked to a diesel forklift activity. On some occasions, increases in particle number concentrations in the worker area and indoor seemed to be related to the use of the diesel forklift while in others this relationship was more difficult to establish. For example, the highest statistically significant increase in mean particle number concentration in the worker area was for SB2, also having the highest percentage of diesel forklift activity 96.2% (Table 2). Moreover, when an increase in number concentration linked to the activity of a diesel forklift was seen in the worker area it was also seen in the outdoor and indoor measurement points. This is probably due to the fact that the diesel forklift was used to load and unload trucks, which means that the forklift was moving from outdoor to indoor having to drive by all the measurement points (worker area, indoor and outdoor). Diesel and propane forklifts have been previously identified as a common source of ultrafine particles (20 – 50 nm) in activities such as warehouse bagging and packing (Ding et al., 2017; Huang et al., 2010; Kuhlbusch et al., 2004; Tsai et al., 2011; Viitanen et al., 2017; Wang et al., 2010).

Finally, in terms of particle mass concentration, no increases when comparing to pre-activity were detected for any of the four days as discussed before. However, during the SB2 packing period, two peaks at 10:40 and 11:30 (Figure 4b) of particles at around 1 μm which coincided with the start of an electric forklift were identified. Huang et al. (2010) observed during packing of large bags (800 kg) that forklift activity released considerable amounts of dust through particle resuspension. In the present case, this phenomenon was only observed on one occasion, and therefore, no clear relationship can be deduced between electric forklift activity and particle mass concentration increases due to resuspension.

3.3. Exposure and risk assessment - Regional inhalation dose rates

Inhalation dose rates were estimated for each day using combined data from NanoScan and MiniWras (Table 3 and S3). Particle number dose rates ($\dot{n}$) during packing ranged between 682×10^6 and 1122×10^6 min^{-1}. Increases (between 87×10^6 and 240×10^6 min^{-1}) during the packing process were obtained when comparing with pre-activity periods for all days. Surface dose ($\dot{s}$) analysis was calculated as well as respiratory tract deposition percentages. From the total surface area of the deposited particles during packing ($3.3 - 7.6 \times 10^6$ µm^2 min^{-1}), 52 – 61% was estimated to deposit in the alveolar region, 13 – 14% in the trachea bronchi and 25 – 36% in the head airways (Table 3). The percentage for the alveolar region is lower than that found by Wang et al. (2010), who determined the percentage of deposited surface area in the alveolar region to be 80% during packing in a carbon black manufacturing industry. No increases in the total surface deposited area during packing were observed when compared with the pre-activity periods except for SB2. In addition, an increase on the percentage on the alveolar and trachea bronchi regions during packing was observed for SB1, whereas for the rest, percentages remained approximately the same. This increase in number and surface deposited area is most likely due to the diesel forklift activity or another process taking place near the packing area and not due to the packing process itself, which emits coarser particles as described in previous sections. The day with the highest percentage of diesel forklift activity (SB2) showed the highest increase in total surface deposited area (4.6×10^6 and 6.0×10^6 µm^2 min^{-1} for pre-activity and process respectively). Higher percentages of deposited particles were detected in the alveolar and head airways regions. Particles deposition on the tracheobronchial area is dominated by particles with diameters under 10 nm. Here, instruments used have an under limit at around 20 nm. Thus, when analyzing tracheobronchial estimations the previous fact must be considered.

463   Particle number deposition percentages on the alveolar region ranged between 66 –

464   69%, similar range as in Wang et al. (2010), who found it to be 64% during packing in a

465   carbon black manufacturing industry. As pointed out in Wang et al. (2010) the use of

466   both metrics, number concentration and surface area, is advisable as, when used

467   separately, different results may be obtained. In Koivisto et al. (2012b) inhalation dose

468   rates as well as percentages of deposited particles in the respiratory tract were

469   calculated for nanoparticle production process in terms of particle number, mass and

470   active surface area. Increases in number concentration and surface area were

471   detected when comparing pre-activity period with process. For that specific case,

472   number concentration was found to be the metric defining better the particles emitted

473   during the process whereas surface area was found to describe process and

474   background particles (Koivisto et al., 2012b).

475   **3.4. Prediction models**

476   Exposure concentrations were modelled using the one and two box models including

477   and excluding outdoor concentrations. Worker area monitored concentrations were

478   compared to one box modelled results, and to FF modelled concentrations when using

479   the two box model, as worker area monitoring instruments were not placed inside the

480   limits of the defined NF area.

481   As described in section 2.4.3, a sensitivity analysis was carried out to identify the

482   optimal air flow rate between NF and FF (β) in the two box model for this industrial

483   setting. The range of values tested was obtained from the literature (Baldwin and

484   Maynard, 1998; Arnold et al., 2017), and the results of this analysis are summarized in

485   Tables 1 and 4. For small bags, a range of S = 0.006-0.05 m s^{-1}, where S is wind

486   speed inside the plant, corresponding to β = 0.36-3 m^3 min^{-1} was tested. Modelled

487   concentrations were seen to variate between 26 and 38%. On the other hand, for big

488   bags a range of S = 0.0125-0.04 m s^{-1} corresponding to β = 9.4-30 m^3 min^{-1} was tested,

489 and modelled concentrations were seen to variate less than 5%. Results evidenced

490 that for small bags, higher β (e.g., 3 m^3 min^{-1}) resulted in modelled/measured ratios up

491 to 1.89, whereas lower β largely underestimated modelled concentrations (ratios =

492 0.39-0.69 for β = 0.36 m^3 min^{-1}). As a result, a β of 0.75 m^3 min^{-1}was selected for the

493 small bag scenarios. In a similar analysis, for the big bag scenarios β was 30 m^3 min^{-1}

494 (Table 1), although as explained β does not seem to be a critical parameter for this

495 scenario.

496 With the parametrization selected, for the one box setup including outdoor

497 concentrations, modelled concentrations (325, 404, 759 and 546 μg m^{-3} for SB1, SB2,

498 BB1 and BB2, respectively) (Table 4) were able to reproduce actual exposure

499 measurements (279, 318, 668 and 528 μg m^{-3} for SB1, SB2, BB1 and BB2,

500 respectively) (Table 3). Predicted concentrations were only slightly higher than the

501 measured values (Table 3 and 4). The ratio ($m_{modelled}/m_{measured}$) was 1.22 ± 0.07 for

502 the small bags and 1.09 ± 0.08 for big bags (Table 4). For the two box model including

503 outdoors, modelled concentrations (311, 316, 745 and 538 μg m^{-3} for SB1, SB1, BB1

504 and BB2, respectively) (Table 4) were higher than measured concentrations with a ratio

505 ($m_{modelled}/m_{measured}$) of 1.05 ± 0.08 for small bags and 1.07 ± 0.07 for big bags

506 (Table 4).

507 Modelled concentrations without adding outdoor concentrations (Table 4) were

508 generally lower than measured concentrations (and only slightly higher in 2 cases; SB1

509 one and two box model including outdoor). The ratio ($m_{modelled}/m_{measured}$) for the one

510 box model was 0.98 ± 0.19 for the small bags and 0.84 ± 0.12 for the big bags. The

511 ratio ($m_{modelled}/m_{measured}$) for the two box model was of 0.88 ± 0.25 for the small

512 bags and 0.82 ± 0.12 for big bags. Thus, the model underestimated exposure

513 concentrations when outdoor contributions were not included. Commonly, model

514 testing assumes that the initial concentration is zero and that the supplied air is free of

contaminants (Zhang et al., 2009). However, as discussed in section 3.3.2, the infiltration of outdoor contaminants is frequent, especially when having open doors as in this case. In the industrial setting under study, modelled concentrations without including outdoor were underestimated in 6 of the 8 cases. This kind of underestimation has been considered detrimental in risk assessment (Arnold et al., 2017). On the other hand, modelled concentrations when including outdoor slightly overestimated measured concentrations and had higher precision. These more conservative results were considered preferable from a risk assessment point of view.

Arnold et al. (2017) highlighted the importance of making the right model selection when applying them to real cases. The use of the two box model in a well-mixed environment can lead to an overestimation of the FF and especially of the NF modeled concentrations, whereas using a one box model to estimate concentrations in a NF-FF environment can lead to an underestimation. In the industrial setting under study, the big bags scenario seemed to be clearly a one box case scenario due to the absence of an enclosure. However, both models provided similar predictions, the one box model resulting in only slightly higher concentrations. In general, overestimation by models has been described for both, one and two box models (Johnson et al., 2011; Koponen et al., 2015; Sahmel et al., 2009).

4. Discussion

Evidently, the results obtained regarding modelled concentrations are highly dependent on model parameters such as the handling energy factor, local controls, air exchange rate (AER) and NF-FF air flow (β), which are not yet fully parametrized (Cherrie et al., 2011; Jayjock et al., 2011; Sahmel et al., 2009; Baldwin and Maynard, 1998; Keil and Zhao, 2017) and are often challenging to estimate (Zhang et al., 2009). Sensitivity analyses such as the one presented in Table 1 are also valuable.

540   In the case of the AER and β, experimental data were not available for this case study

541   and they were thus obtained from the literature and tested by means of a sensitivity

542   analysis. β was seen to be a key parameter when modelling the small bags case

543   scenario while it is not critical for the big bags case scenario. That may be explained by

544   the fact that the small bags case scenario was a real two box case (with an actual

545   enclosure and with a small surface area for the air flow between NF and FF) whereas

546   for the big bags there was no real separation between NF and FF and consequently

547   the theoretical free surface area used in the model was much higher.

548   Local controls prevent dispersion of the aerosolized particles in the room air or remove

549   the particles from air, e.g. enclosures or local extraction systems (Fransman et al.,

550   2008). When having to consider extractions systems, local control values associated

551   can be relatively easy to determine, but in cases like enclosures or barriers it is more

552   complex especially without having actual exposure concentrations. Local exhaust

553   ventilation efficiency can be calculated by a relatively simple equation (Hewett and

554   Ganser, 2017) although some unknown parameters are required. For cases such as

555   the present study when there is no possibility to experimentally establish a value,

556   Fransman et al. (2008) conducted a review with values proposed for different local

557   controls. Here, enclosure local control and bag protection was included in the equation

558   by using values reviewed in Fransman et al. (2008). The output modelled

559   concentrations were seen to correctly predict measured concentrations when using the

560   reported values.

561   Finally, the emission source characterization is one of the main sources of uncertainty

562   in the model, as it is strongly case-specific. This is one of the reasons why studies

563   dealing with real-world scenarios are highly necessary in the literature. As in the

564   present study, emission source characterization can be based on the dustiness index

565   which may be obtained by standard methods (Lidén, 2006). However, the handling

566   energy factor must be considered (Koivisto et al., 2015; Lidén, 2006; Schneider and

567 Jensen, 2007). When the dustiness concept cannot be used, equations to estimate

568 emission rates have been described (Hewett and Ganser, 2017; Sachse et al., 2012)

569 and used on real scenarios by using mass equation balance and a convolution theorem

570 (Koivisto et al., 2018a; Koivisto et al., 2018b). However, unlike the other parameters,

571 literature regarding emission rates is still limited.

572 Additionally, an important consideration to be discussed at this point is that the models

573 do not consider particle losses due to sedimentation. Cherrie et al. (2011) found that for

574 particles < 10 μm the impact of deposition might be reasonably ignored, but for

575 particles with a higher aerodynamic diameter the deposition impact may be important.

576 Figure 5 shows that most of the emitted particles during packing were under 10 μm.

577 However, for BB1, a slight increase of particles > 10 μm during packing was observed.

578 Based on the considerations above, it may be concluded that the use of the one box

579 and two box models in the industrial setting tested can satisfactorily predict particle

580 concentrations, especially when input parameters are sufficiently robust. In Sahmel et

581 al. (2009), the steady state model, similar to the one box model used here, was seen to

582 correctly perform concentration modeling when choosing the appropriate factors.

583 However, in industrial settings many considerations must be taken into account and

584 what is clearly observed in a laboratory scale or controlled settings cannot be directly

585 extrapolated to the industrial world. To this end, the parameters used in this work and

586 the coefficients applied, described in section 2.4, may be useful as input for future

587 modelling studies.

588 **5. Conclusions**

589 Packing of a fertilizer into small (respirable fraction range 279-318 μg m^{-3}) and big bags

590 (respirable fraction range 487-668 μg m^{-3}) was not seen to significantly increase worker

591 exposure compared with pre-activity concentrations in terms of inhalable and respirable

592 concentrations. However, increases in particle number concentrations were observed,

593 quite likely related to the diesel forklift activity. A statistically significant increase in

594 ultrafine particles was observed for SB2 (58646 cm^{-3} during pre-activity; 75912 cm^{-3}

595 during packing). This dataset was used to test the performance of one and two box

596 models as tools for risk assessment under real-world industrial settings.

597 The one and two box models were tested in a real industrial exposure case scenario,

598 during packing of a fertilizer into small and big bags, with and without enclosure. Both

599 models seemed to be able to predict exposure concentrations. When outdoor

600 concentrations were not included in the models, modelled concentrations slightly

601 underestimated actual concentrations, with ratios modelled/measured ranging between

602 0.82 ± 0.12 and 0.98 ± 0.19 for the respirable size fraction. The use of outdoor

603 concentrations as an input for the models was seen to improve model performance,

604 resulting in slight overestimations of measured concentrations what was estimated as

605 preferable from a risk assessment point of view. In addition, higher precision between

606 repetitions was achieved when including outdoor contributions (ratio

607 modelled/measured 1.05 ± 0.08 to 1.22 ± 0.07). Thus, it was concluded that including

608 outdoor concentrations in the model resulted in an improved model performance, which

609 may be considered a step forward in the application of risk assessment models.

610 With regard to the selection of the one or two box models, similar results for the small

611 and big bags case scenarios were obtained. However, slightly better results were

612 obtained when using the two box model for the small bags scenario (one box model

613 1.22 ± 0.07; two box model 1.05 ± 0.08), whereas both models provided similar results

614 for the big bags (1.09 ± 0.08 and 1.07 ± 0.07 respectively). Thus, it may be concluded

615 that, even in complex real-world settings, the simplest approach of the one box model

616 may provide good results if it is adequately parametrized. Model parametrization is in

617 itself a key issue: the selection of parameters such as the handling energy factor, the

618 local controls and especially the NF-FF air flow in the two box model were seen to be

619 critical for the model's performance. Here, NF-FF air flow, local controls efficiency as

620 well as handling energy factor were assumed based on literature databases, and

621 relatively accurate predictions were obtained. Therefore, reporting measured or tested

622 values for these parameters is seen as necessary to expand the use and applicability

623 of prediction models for risk assessment.

624 **5. Acknowledgments**

633 **References**

634 Arnold, S.F., Shao, Y., Ramachandran, G., 2017. Evaluating well-mixed room and

635   near-field–far-field model performance under highly controlled conditions. J.

636   Occup. Environ. Hyg. 14, 427–437.

637 Asbach, C., Kuhlbusch, T.A.J., Kaminski, H., Stahlmecke, B., Plitzko, S., Götz, U.,

638   Voetz, M., Kiesling, H.-J., Dahmann, D., 2012. Standard Operation Procedures

639   For assessing exposure to nanomaterials, following a tiered approach.

640 Baldwin, P.E.J., Maynard, A.D., 1998. A Sonirvey of Wnnnd Speeds Inn Imioor

641   Workplaces 42, 303–313.

642 Bennett, D.H., Koutrakis, P., 2006. Determining the infiltration of outdoor particles in

643   the indoor environment using a dynamic model. Aerosol Sci. 37, 766–785.

644 Boelter, F.W., Simmons, C.E., Berman, L., Scheff, P., 2009. Two-zone model

645   application to breathing zone and area welding fume concentration data. J. Occup.

646   Environ. Hyg. 6, 289–297.

647 Cherrie, J.W., MacCalman, L., Fransman, W., Tielemans, E., Tischer, M., Van

648   Tongeren, M., 2011. Revisiting the effect of room size and general ventilation on

649   the relationship between near- and far-field air concentrations. Ann. Occup. Hyg.

650   55, 1006–1015.

651 Cousins, C., Boice Jr, J., Cooper, U.J., Lee, U.J., Lochard, K.J., 2011. Annals of the

652   ICRP Published on behalf of the International Commission on Radiological

653   Protection International Commission on Radiological Protection Members of the

654   2010–2013 Main Commission of ICRP.

655 Ding, Y., Kuhlbusch, T.A.J., Van Tongeren, M., Jiménez, A.S., Tuinman, I., Chen, R.,

656   Alvarez, I.L., Mikolajczyk, U., Nickel, C., Meyer, J., Kaminski, H., Wohlleben, W.,

657   Stahlmecke, B., Clavaguera, S., Riediker, M., 2017. Airborne engineered

658   nanomaterials in the workplace—a review of release and worker exposure during

659   nanomaterial production and handling processes. J. Hazard. Mater. 322, 17–28.

660 European Committee for Standardization (CEN), 2013. Workplace exposure:

661   Measurement of the dustiness of bulk materials; Part1: Requirements and choice

662   of test methods; Part 2: Rotating drum method; Part 3: Continuous drop method

663   (EN 15051). [Stantdard] Brussels, Belgium, 2013.

664 Evans, D.E., Ku, B.K., Birch, M.E., Dunn, K.H., 2010. Aerosol Monitoring during

665   Carbon Nanofiber Production: Mobile Direct-Reading Sampling. Ann. Occup. Hyg.

666   54, 514–531.

667 Fonseca, A.S., Viana, M., Pérez, N., Alastuey, A., Querol, X., Kaminski, H., Todea,

668   A.M., Monz, C., Asbach, C., 2016. Intercomparison of a portable and two

669   stationary mobility particle sizers for nanoscale aerosol measurements. Aerosol

670   Sci. Tech. 50, 653–668.

671 Fransman, W., Schinkel, J., Meijster, T., Van Hemmen, J., Tielemans, E., Goede, H.,

672   2008. Development and evaluation of an Exposure Control Efficacy Library

673   (ECEL). Ann. Occup. Hyg. 52, 567–575.

674 Fujitani, Y., Kobayashi, T., Arashidani, K., Kunugita, N., Suemura, K., 2008.

675   Measurement of the Physical Properties of Aerosols in a Fullerene Factory for

676   Inhalation Exposure Assessment. J. Occup. Environ. Hyg. 5, 380–389.

677 Global, regional, and national comparative risk assessment of 84 behavioural,

678   environmental and occupational, and metabolic risks or clusters of risks, 1990–

679   2016: a systematic analysis for the Global Burden of Disease Study 2016. Lancet

680   390, 1345–1422.

681 Ganser, G.H., Hewett, P., 2017. Models for nearly every occasion: Part II - Two box

682   models. J. Occup. Environ. Hyg. 14, 58–71.

683 Heitbrink, W.A., Evans, D.E., Ku, B.K., Maynard, A.D., Slavin, T.J., Peters, T.M., 2009.

684   Relationships among particle number, surface area, and respirable mass

685   concentrations in automotive engine manufacturing. J. Occup. Environ. Hyg. 6,

686   19–31.

687 Hewett, P., Ganser, G.H., 2017. Models for nearly every occasion: Part I - One box

688   models. J. Occup. Environ. Hyg. 14, 49–57.

689 Hinds, W.C., 1999. Aerosol technology: Properties, Behavior, and Measurement of

690   Airborne Particles., Wiley-Interscience Publication. Wiley.

691 Huang, C.H., Tai, C.Y., Huang, C.Y.U., Tsai, C.J., Chen, C.W., Chang, C.P., Shih,

692   T.S., 2010. Measurements of respirable dust and nanoparticle concentrations in a

693   titanium dioxide pigment production factory. J. Environ. Sci. Heal. - Part A

694   Toxic/Hazardous Subst. Environ. Eng. 45, 1227–1233.

695   Hussein, T., Hruška, A., Dohányosová, P., Džumbová, L., Hemerka, J., Kulmala, M.,

696   Smolík, J., 2009. Deposition rates on smooth surfaces and coagulation of aerosol

697   particles inside a test chamber. Atmos. Environ. 43, 905–914.

698   Hussein, T., Kulmala, M., 2008. Indoor Aerosol Modeling: Basic Principles and

699   Practical Applications. Water, Air, Soil Pollut. Focus 8, 23–34.

700   ICSC 0184 - POTASSIUM NITRATE [WWW Document], n.d. URL

701   http://www.inchem.org/documents/icsc/icsc/eics0184.htm (accessed 1.26.18).

702   INSH, 2018. LEP 2018, Instituto Nacional de Seguridad e Higiene en el Trabajo.

703   Jayjock, M.A., Armstrong, T., Taylor, M., 2011. The daubert standard as applied to

704   exposure assessment modeling using the two-zone (NF/FF) model estimation of

705   indoor air breathing zone concentration as an example. J. Occup. Environ. Hyg. 8,

706   D114–D122.

707   Johnson, M., Lam, N., Brant, S., Gray, C., Pennise, D., 2011. Modeling indoor air

708   pollution from cookstove emissions in developing countries using a Monte Carlo

709   single-box model. Atmos. Environ. 45, 3237–3243.

710   Jones, R.M., Simmons, C.E., Boelter, F.W., 2011. Comparing two-zone models of dust

711   exposure. J. Occup. Environ. Hyg. 8, 513–519.

712   Kaminski, H., Beyer, M., Fissan, H., Asbach, C., Kuhlbusch, T.A.J., 2015.

713   Measurements of nanoscale TiO2 and Al2O3 in industrial workplace

714   environments -Methodology and results. Aerosol Air Qual. Res. 15, 129–141.

715   Kleinman, M.T., Linn, W.S., Bailey, R.M., Jones, M.P., Hackney, J.D., 1980. Effect of

716   ammonium nitrate aerosol on human respiratory function and symptoms. Environ.

717   Res. 21, 317–326.

718   Koivisto, A.J., Lyyränen, J., Auvinen, A., Vanhala, E., Hämeri, K., Tuomi, T., Jokiniemi,

719   J., 2012a. Industrial worker exposure to airborne particles during the packing of

720   pigment and nanoscale titanium dioxide. Inhal. Toxicol. 24, 839–849.

721 Koivisto, A.J., Aromaa, M., Mäkelä, J.M., Pasanen, P., Hussein, T., Hämeri, K., 2012b.

722   Concept To Estimate Regional Inhalation Dose of Industrially Synthesized

723   Nanoparticles. ACSNano 6, 1195–1203.

724 Koivisto, A.J., Jensen, A.C.Ø., Kling, K.I., Kling, J., Budtz, H.C., Koponen, I.K.,

725   Tuinman, I., Hussein, T., Jensen, K.A., Nørgaard, A., Levin, M., 2018. Particle

726   emission rates during electrostatic spray deposition of TiO 2 nanoparticle-based

727   photoactive coating. J. Hazard. Mater. 341, 218–227.

728 Koivisto, A.J., Jensen, A.C.Ø., Levin, M., Kling, K.I., Maso, M.D., Nielsen, S.H.,

729   Jensen, K.A., Koponen, I.K., 2015. Testing the near field/far field model

730   performance for prediction of particulate matter emissions in a paint factory.

731   Environ. Sci. Process. Impacts 17, 62–73.

732 Koivisto, A.J., Kling, K.I., Fonseca, A.S., Bluhme, A.B., Moreman, M., Yu, M., Costa,

733   A.L., Giovanni, B., Ortelli, S., Fransman, W., Vogel, U., Jensen, K.A., 2018. Dip

734   coating of air purifier ceramic honeycombs with photocatalytic TiO 2 nanoparticles:

735   A case study for occupational exposure. Sci. Total Environ. 630, 1283–1291.

736 Koponen, I.K., Asmi, A., Keronen, P., Puhto, K., Kulmala, M., 2001. Indoor air

737   measurement campaign in Helsinki, Finland 1999 - The effect of outdoor air

738   pollution on indoor air. Atmos. Environ. 35, 1465–1477.

739 Koponen, I.K., Koivisto, A.J., Jensen, K.A., 2015. Worker exposure and high time-

740   resolution analyses of process-related submicrometre particle concentrations at

741   mixing stations in two paint factories. Ann. Occup. Hyg. 59, 749–763.

742 Kuhlbusch, T.A.J., Neumann, S., Fissan, H., 2004. Number Size Distribution, Mass

743   Concentration, and Particle Composition of PM $_1$, PM $_{2.5}$, and PM $_{10}$ in Bag Filling

744   Areas of Carbon Black Production. J. Occup. Environ. Hyg. 1, 660–671.

745   Landrigan, P.J., Fuller, R., Acosta, N.J.R., Adeyi, O., Arnold, R., Basu, N., Baldé, A.B.,

746   Bertollini, R., Bose-O'Reilly, S., Boufford, J.I., Breysse, P.N., Chiles, T., Mahidol,

747   C., Coll-Seck, A.M., Cropper, M.L., Fobil, J., Fuster, V., Greenstone, M., Haines,

748   A., Hanrahan, D., Hunter, D., Khare, M., Krupnick, A., Lanphear, B., Lohani, B.,

749   Martin, K., Mathiasen, K. V, McTeer, M.A., Murray, C.J.L., Ndahimananjara, J.D.,

750   Perera, F., Potočnik, J., Preker, A.S., Ramesh, J., Rockström, J., Salinas, C.,

751   Samson, L.D., Sandilya, K., Sly, P.D., Smith, K.R., Steiner, A., Stewart, R.B., Suk,

752   W.A., van Schayck, O.C.P., Yadama, G.N., Yumkella, K., Zhong, M., 2017. The

753   Lancet Commission on pollution and health. Lancet 391.

754   Lidén, G., 2006. Dustiness testing of materials handled at workplaces. Ann. Occup.

755   Hyg. 50, 437–339.

756   López-Lilao, A., Bruzi, M., Sanfélix, V., Gozalbo, A., Mallol, G., Monfort, E., 2015.

757   Evaluation of the Dustiness of Different Kaolin Samples. J. Occup. Environ. Hyg.

758   12, 547–554.

759   Lopez, R., Lacey, S.E., Jones, R.M., 2015. Application of a Two-Zone Model to

760   Estimate Medical Laser-Generated Particulate Matter Exposures. J. Occup.

761   Environ. Hyg. 12, 309–313.

762   Gorguner, M.A., 2003. Acute inhalation injury. Emerg. Med. Clin. North Am. 21, 533–

763   557.

764   Nazaroff, W.W., 2004. Indoor particle dynamics. Indoor Air 14, 175–183.

765   Nazaroff, W.W., Cass, G.R., 1989. Mathematical modeling of indoor aerosol dynamics.

766   Environ. Sci. Technol. 23, 157–166.

767   Nicas, M., 2016. The near field/far field model with constant application of chemical

768   mass and exponentially decreasing emission of the mass applied. J. Occup.

769   Environ. Hyg. 13, 519–528.

770   Notø, H., Nordby, K.-C., Skare, Ø., Eduard, W., 2018. Job Tasks as Determinants of

771   Thoracic Aerosol Exposure in the Cement Production Industry. Ann. Work Expo.

772   Heal. 62, 88–100.

773   Peters, T.M., Elzey, S., Johnson, R., Park, H., Grassian, V.H., Maher, T.,

774   O'Shaughnessy, P., 2008. Airborne Monitoring to Distinguish Engineered

775   Nanomaterials from Incidental Particles for Environmental Health and Safety. J.

776   Occup. Environ. Hyg. 6, 73–81.

777   Pujara, C.P., 1997. Determination of factors that affect the generation of airborne

778   particles from bulk pharmaceutical powders. PhD diss., Purdue Univeristy, USA.

779   Reche, C., Viana, M., Rivas, I., Bouso, L., Àlvarez-Pedrerol, M., Alastuey, A., Sunyer,

780   J., Querol, X., 2014. Outdoor and indoor UFP in primary schools across

781   Barcelona. Sci. Total Environ. 493, 943–953.

782   Ribalta, C., Viana, M., López-Lilao, A., Estupiñá, S., Minguillón, M.C., Mendoza, J.,

783   Díaz, J., Dahmann, D., Monfort, E., 2018 under review. On the relationships

784   between exposure to particles and dustiness during handling of powders in

785   industrial settings. Ann. Work Expo.

786   Rivas, I., Viana, M., Moreno, T., Bouso, L., Pandolfi, M., Alvarez-Pedrerol, M., Forns,

787   J., Alastuey, A., Sunyer, J., Querol, X., 2015. Outdoor infiltration and indoor

788   contribution of UFP and BC, OC, secondary inorganic ions and metals in PM2.5 in

789   schools. Atmos. Environ. 106, 129–138.

790   Sachse, S., Silva, F., Irfan, A., Zhu, H., Pielichowski, K., Leszczynska, A., Blazquez,

791   M., Kazmina, O., Kuzmenko, O., Njuguna, J., 2012. Physical characteristics of

792   nanoparticles emitted during drilling of silica based polyamide 6 nanocomposites.

793   IOP Conf. Ser. Mater. Sci. Eng. 40, 12012.

794   Sahmel, J., Unice, K., Scott, P., Cowan, D., Paustenbach, D., 2009. The use of

795   multizone models to estimate an airborne chemical contaminant generation and

796   decay profile: Occupational exposures of hairdressers to vinyl chloride in hairspray

797   during the 1960s and 1970s. Risk Anal. 29, 1699–1725.

798   Schneider, T., Jensen, K.A., 2007. Combined Single-Drop and Rotating Drum

799   Dustiness Test of Fine to Nanosize Powders Using a Small Drum. Ann. Occup.

800   Hyg. 52, 23–34.

801   Shruthi N, A.B. and S.M., 2017. Toxic effect of inorganic fertilizers to earthworms

802   (Eudrilus eugeniae). J. Entomol. Zool. Stud. JEZS 5, 1135–1137.

803   Tsai, C.J., Huang, C.Y., Chen, S.C., Ho, C.E., Huang, C.H., Chen, C.W., Chang, C.P.,

804   Tsai, S.J., Ellenbecker, M.J., 2011. Exposure assessment of nano-sized and

805   respirable particles at different workplaces. J. Nanoparticle Res. 13, 4161–4172.

806   Tsimakuridze, M., Saakadze, V., Tsereteli, M., 2005. [The characteristic state of health

807   of ammonia nitrate producing workers]. Georg. Med News 80–83.

808   Van Broekhuizen, P., Van Veelen, W., Streekstra, W.H., Schulte, P., Reijnders, L.,

809   2012. Exposure limits for nanoparticles: Report of an international workshop on

810   nano reference values, in: Annals of Occupational Hygiene. Edinburgh Napier

811   University, pp. 515–524.

812   Viitanen, A.K., Uuksulainen, S., Koivisto, A.J., Hämeri, K., Kauppinen, T., 2017.

813   Workplace measurements of ultrafine particles-A literature review. Ann. Work

814   Expo. Heal.

815   Wang, J., Asbach, C., Fissan, H., Hülser, T., Kaminski, H., Kuhlbusch, T.A.J., Pui,

816   D.Y.H., 2012. Emission measurement and safety assessment for the production

817   process of silicon nanoparticles in a pilot-scale facility. J. Nanoparticle Res. 14,

818   759.

819   Wang, Y.F., Tsai, P.J., Chen, C.W., Chen, D.R., Hsu, D.J., 2010. Using a modified

820   electrical aerosol detector to predict nanoparticle exposures to different regions of

821   the respiratory tract for workers in a carbon black manufacturing industry. Environ.

822   Sci. Technol. 44, 6767–6774.

823   World Health Organization, 2016. Ambient Air Pollution: A global assessment of

824   exposure and burden of disease. World Heal. Organ. 1–131.

825   Zhang, Y., Banerjee, S., Yang, R., Lungu, C., Ramachandran, G., 2009. Bayesian

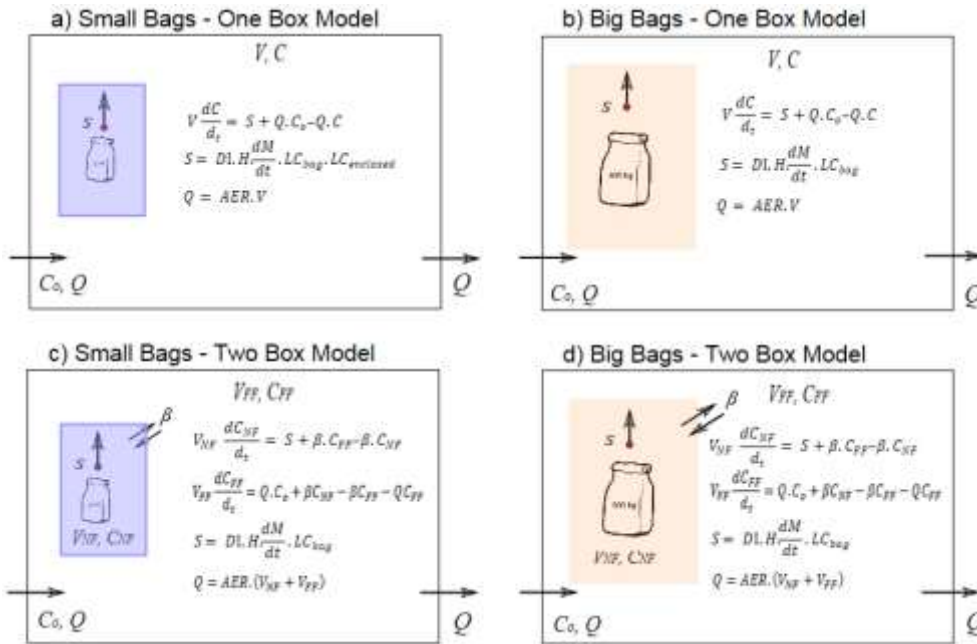826   modeling of exposure and airflow using two-zone models. Ann. Occup. Hyg.

827

828   **Figures and Tables**
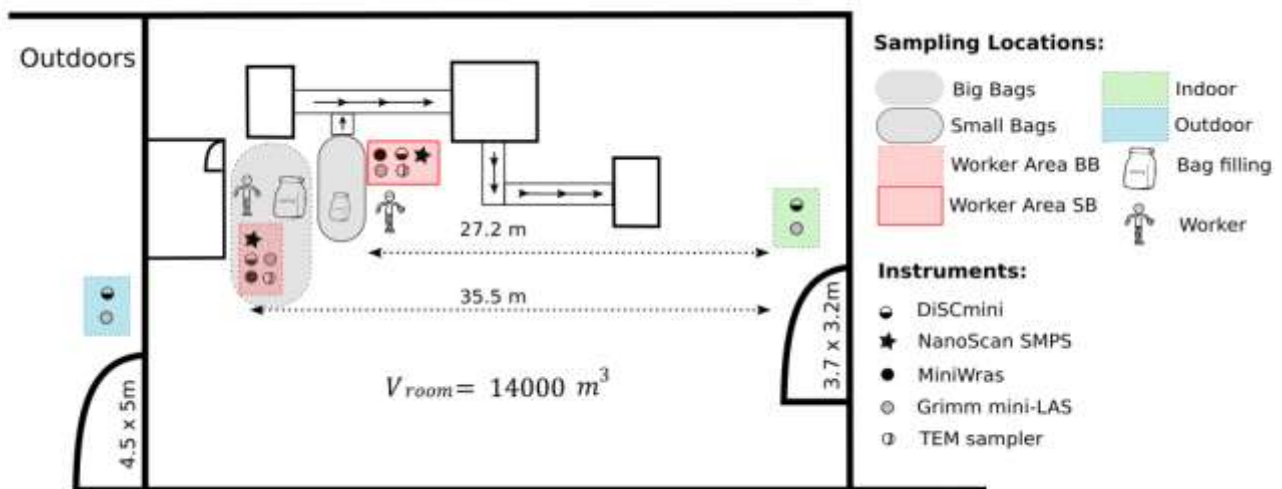
829

830   **Figure 1**. Packing industrial unit layout. Measurement locations as well as devices used during packing

831   operation are pointed out. BB: big bags. SB: small bags.

832

SMALL BAGS

Respirable dustness index	DI	16 mg/kg	Very low dustness index
Mass flow	dM/dt	250 kg/min	Mass flow value
Handling energy	H	0.5	Drop height is approximately half of the dustness test drop height
Local emission controls	LC_{bag}	0.6	0.6 = bag acts as a protection (reduction of the emissions of a 40%)
	$LC_{enclosed}$	0.5	0.5 = process enclosed (reduction of the emissions of a 50%)
Room volume	V_{room}/V_{FF}	14000 m^3	Big industrial unit
Air Exchange rate	AER	7 ACH	Medium ventilation rate
Near field volume	V_{NF}	6 m^3	Volume of the enclosed space, it does not include the worker area
Near field air flow	β	0.75 m^3/min	Low air exchange NF-FF (enclosed process)

BIG BAGS

Respirable dustness index	DI	16 mg/kg	Very low dustness index
Mass flow	dM/dt	175 kg/min	Mass flow value
Handling energy	H	1	1 is equivalent to the drop height in the dustness test
Local emission controls	LC_{bag}	0.6	0.6 = bag acts as a protection (reduction of the emissions of a 40%)
Room volume	V_{room}/V_{FF}	14000 m^3	Big industrial unit
Air Exchange rate	AER	7 ACH	Medium ventilation rate
Near field volume	V_{NF}	25m^3	Volume of the bagging line area including worker area
Near field air flow	β	30 m^3/min	High air exchange NF-FF (opened process)

833 **Figure 2**. One box and two box model description and parameters values (table). For small bags, one box
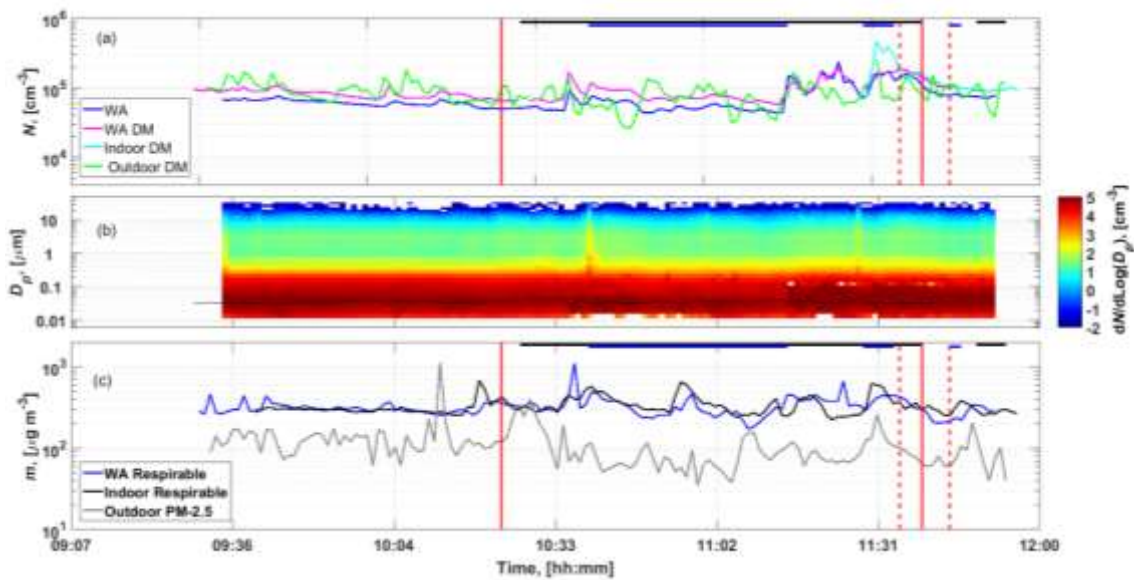
834 model (a) and two box model (c) and for big bags, one box model (b) and two box model (d).

835

836
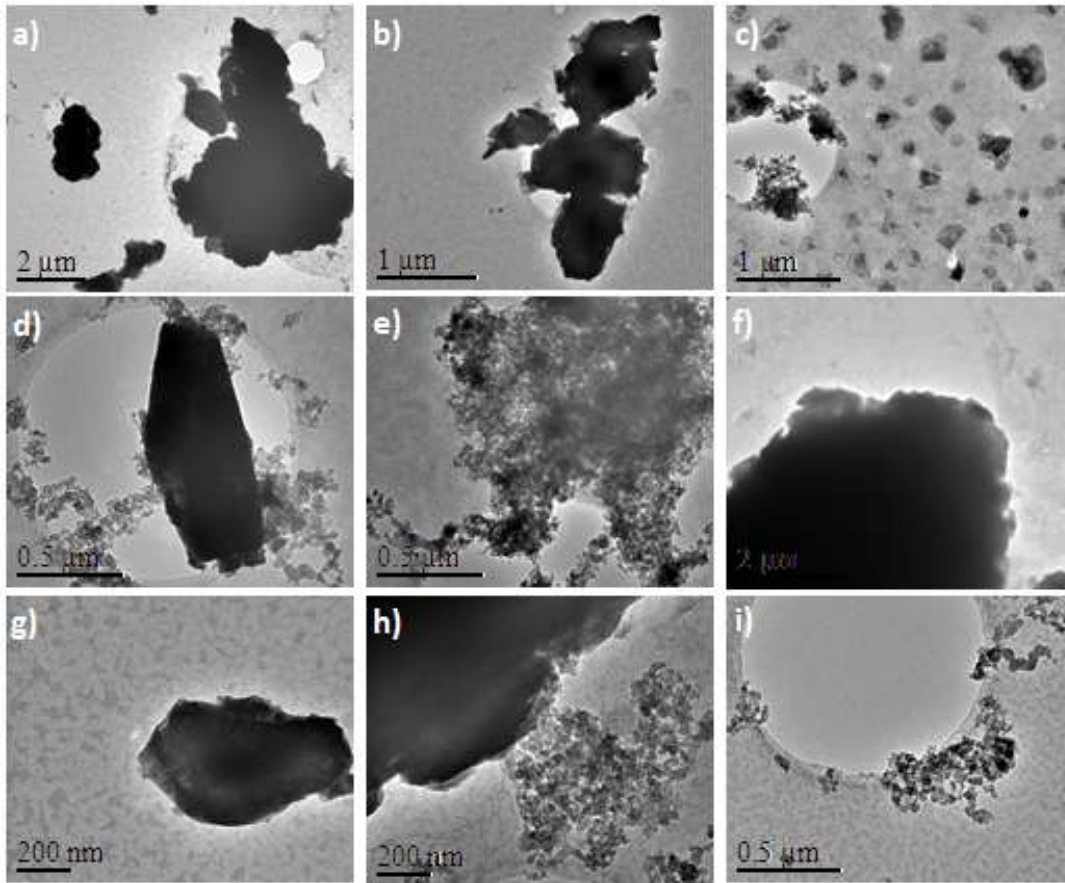
Figure 3. TEM images of the colected particles during the fertilizer bag filling process with small (a, b, c, d and e), and big bags (f, g, h and i).

839

Figure 4. Particle concentration at packing area (WA) during small bags 2 (SB2): (a) particle number concentration time series; (b) particle size distribution time series measured with the MiniWras and the NanoScan, solid black line shows DiSCmini (DM) D_{50}; (c) mass concentration time series. Red vertical

843   lines indicate start (solid line) and stop (dashed line) of the packing operation and horizontal black and

844   blue lines in the top of the graphs indicate diesel and electric forklifts activity respectively.
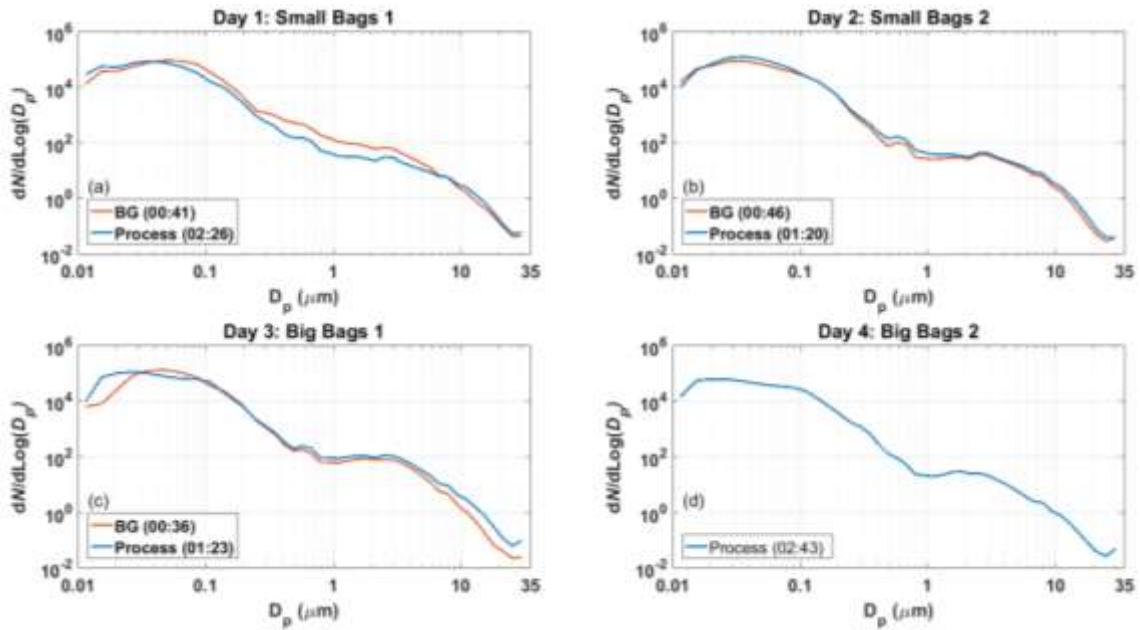
845

846   **Figure 5.** Average particle size distributions measured by NanoScan and MiniWras during pre-activity and

847   packing processes for (a) small bags day 1, SB1; (b) small bags day 2, SB2; (c) big bags day 1, BB1 and

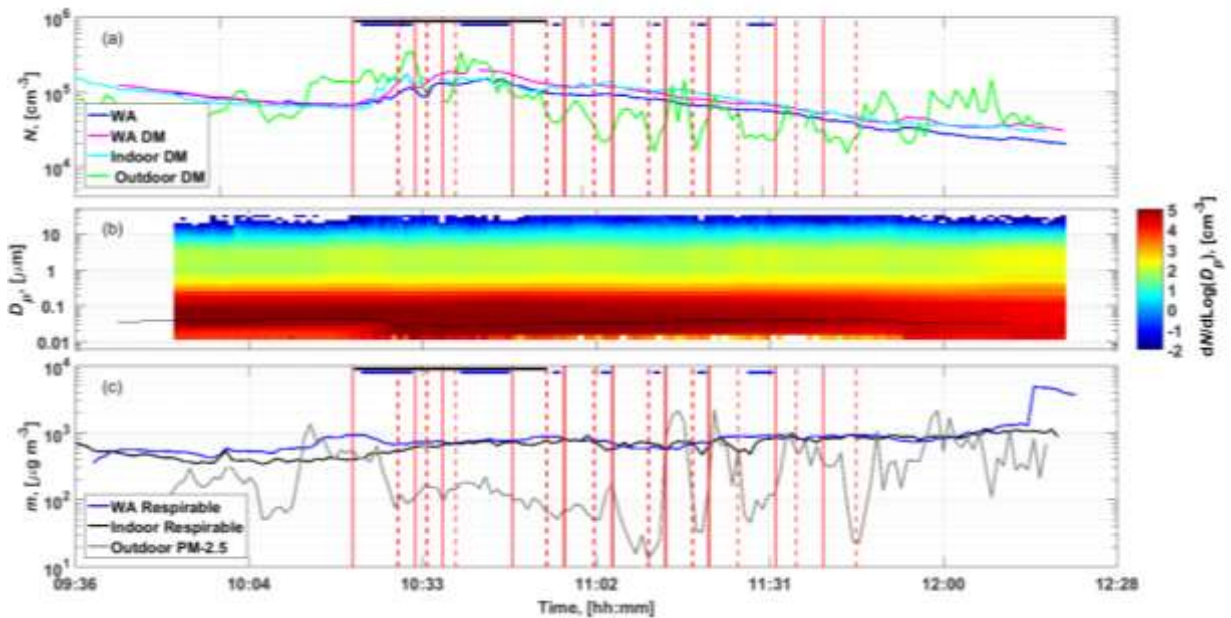848   (d) big bags day 2, BB2.

849

850   **Figure 6.** Particle concentration at packing area (WA) during big bags day 1 (BB1): (a) particle number

851   concentration time series; (b) particle size distribution time series measured with the MiniWras and the

852   NanoScan, solid black line shows DiSCmini (DM) D_{50}; (c) mass concentration time series. Red vertical

lines indicate start (solid line) and stop (dashed line) of the packing operation and horizontal black and blue lines in the top of the graphs indicate diesel and electric forklifts activity respectively.

Table 1. Sensitivity analysis for different air flow values for small and big bags with ratios (modelled values/measured values). Variation (%) of the modelled concetration when using the higher and lower air flow value is reported. $\beta = \frac{1}{2}. \; SA . S; where \; SA \; is \; the \; surface \; area.$

β (m³ min⁻¹)	S (m s⁻¹)	SB1 With outdoor Ratio	SB1 Ratio	SB2 With outdoor Ratio	SB2 Ratio	β (m³ min⁻¹)	S (m s⁻¹)	BB1 With outdoor Ratio	BB1 Ratio	BB2 With outdoor Ratio	BB2 Ratio
0.36	0.006	0.69	0.63	0.68	0.39	-	-	-	-	-	-
0.5	0.004	0.87	0.81	0.81	0.51	-	-	-	-	-	-
0.75	0.0125	1.11	1.06	0.99	0.70	9.4	0.0125	1.08	0.70	0.99	0.88
1	0.017	1.30	1.25	1.15	0.86	12.75	0.017	1.10	0.71	1.00	0.89
1.5	0.025	1.56	1.50	1.40	1.1	15	0.02	1.10	0.71	1.01	0.90
1.8	0.03	1.66	1.60	1.51	1.21	-	-	-	-	-	-
2.4	0.04	1.80	1.75	1.67	1.36	30	0.04	1.12	0.73	1.02	0.91
3	0.05	1.89	1.84	1.79	1.50	-	-	-	-	-	-
Variation (%)		36.4	34.6	38.0	25.8	Variation (%)		3.0	4.5	2.6	2.9

Table 2. Pre-activity, total process time, and total time for each activity (packing, electric forklift and diesel forklift) shown in hh:mm. The percentage of time of each activity (packing, electric forklift and diesel forklift) with respect to the total lenght of the process is included in brackets. Background period (pre-activity) not included. Less than 5 minutes difference between stop and start of the next activity was counted as the same period activity.

Process	Background time	Packing process time	Material pouring time (%)	Electric forklift time (%)	Diesel forklift time (%)
SB1	00:41	02:26	02:03 (84.2%)	00:02 (1.4%)	00:44 (30.2%)
SB2	00:46	01:20	01:16 (95.0%)	00:42 (53.2%)	01:17 (96.2%)
BB1	00:36	01:23	00:46 (55.9%)	00:26 (32.1%)	00:31 (38.4%)
BB2	-	02:43	00:36 (22.1%)	00:40 (24.9%)	02:05 (77.1%)

37

864 **Table 3.** Mean number concentration and mass concentrations during background period (BG) (pre-
865 activity) and packing process in the worker area (WA). N_{TOT} (Dp: 10 nm – 35 μm), N_{UPF} (Dp <; 86.60 nm),
866 N_{FP} (86.60 nm < Dp < 943.0 nm), N_C (Dp> 943.0 nm). Mass concentrations are shown in terms of
867 inhalable, thoracic and respirable fractions measured with the Grimm monitor. Calculated dose rates in
868 particle number, $\dot{n}$, and surface area, $\dot{s}$, and regional deposition in percentages on head airways, trachea
869 bronchi and alveolar. Values in bold indicate statistically significant differences compared with background
870 concentrations.

	Small Bags day 1 (SB1)		Small Bags day 2 (SB2)		Big Bags day 1 (BB1)		Big Bags day 2 (BB2)	
	BG	Packing	BG	Packing	BG	Packing	BG	Packing
N_{TOT} [cm^{-3}]	67254 ± 11076	63108 ± 29592	63797 ± 5435	**81137 ± 42448**	81073 ± 8719	85949 ± 29748	-	50290 ± 40893
N_{UPF} [cm^{-3}]	61083	59900	58646	**75912**	73641	77945	-	46359
N_{FP} [cm^{-3}]	6121	**3188**	5129	5197	7383	7935	-	3922
N_C [cm^{-3}]	50	**20**	22	**28**	50	**68**	-	14
Inhalable [μg m^{-3}]	1987 ± 214	2025 ± 975	1866 ± 1141	1276 ± 550	1650 ± 588	1864 ± 556	-	1047 ± 923
Thoracic [μg m^{-3}]	1487 ± 138	**1053 ± 435**	1147 ± 315	962 ± 345	1183 ± 367	1507 ± 381	-	787 ± 721
Respirable [μg m^{-3}]	634 ± 64	**279 ± 131**	362 ± 74	318 ± 109	354 ± 105	668 ± 153	-	528 ± 898
$\dot{n}, \cdot 10^6$ [min^{-1}]	770	857	834	1035	882	1122	-	682
$\dot{s}, \cdot 10^6$ [μm^2 min^{-1}]	6.4	4.3	4.6	6.0	7.5	7.6	-	3.3
$\dot{s}$.Head airways [%]	30.7	26.3	27.1	26.2	28.0	36.0	-	24.7
$\dot{s}$.Trachea bronchi [%]	12.7	14.2	13.9	14.0	13.3	12.5	-	14.2
$\dot{s}$.Alveolar [%]	56.6	59.5	59.0	59.8	58.7	51.5	-	61.1

871

872

873

874

875   **Table 4.** One box and two box modeled respirable concentration results including and without including

876   outdoor concentrations. Ratios between modeled and measured concentrations for each specific case are

877   shown in brackets. Last two columns are mean ratio values (and standard deviation) for small and big

878   bags (SB and BB). Last row shows the measured respirable fraction concentrations in the workers area

879   and the spatial background.

$[\mu g/m^3]$ (ratio $_{modelled/measured}$)	SB1	SB2	BB1	BB2	Ratio mean ± (s.d)	
					Small bags	Big bags
One box with outdoor	325 (1.16)	404 (1.27)	759 (1.14)	546 (1.03)	1.22 (0.07)	1.09 (0.08)
Two box with outdoor (FF)	311 (1.11)	316 (0.99)	745 (1.12)	538 (1.02)	1.05 (0.08)	1.07 (0.07)
One box	310 (1.11)	270 (0.85)	501 (0.75)	488 (0.92)	0.98 (0.19)	0.84 (0.12)
Two box (FF)	296 (1.06)	223 (0.70)	487 (0.73)	480 (0.90)	0.88 (0.25)	0.82 (0.12)
Measured respirable fraction in Worker Area	279	318	668	528	-	

880

881